

# Exploration of the Potential Energy Surface of $C_9H_9^+$ by ab Initio Methods. 2. Is the 1,4-Bishomotropylium Cation a Bishomoaromatic Prototype?

Dieter Cremer,<sup>\*,†</sup> Peder Svensson,<sup>‡</sup> Elfi Kraka,<sup>†</sup> Zoran Konkoli,<sup>†</sup> and Per Ahlberg<sup>\*,‡</sup>

Contribution from the Departments of Theoretical Chemistry and Organic Chemistry, University of Göteborg, Kemigården 3, S-41296 Göteborg, Sweden

Received October 16, 1992

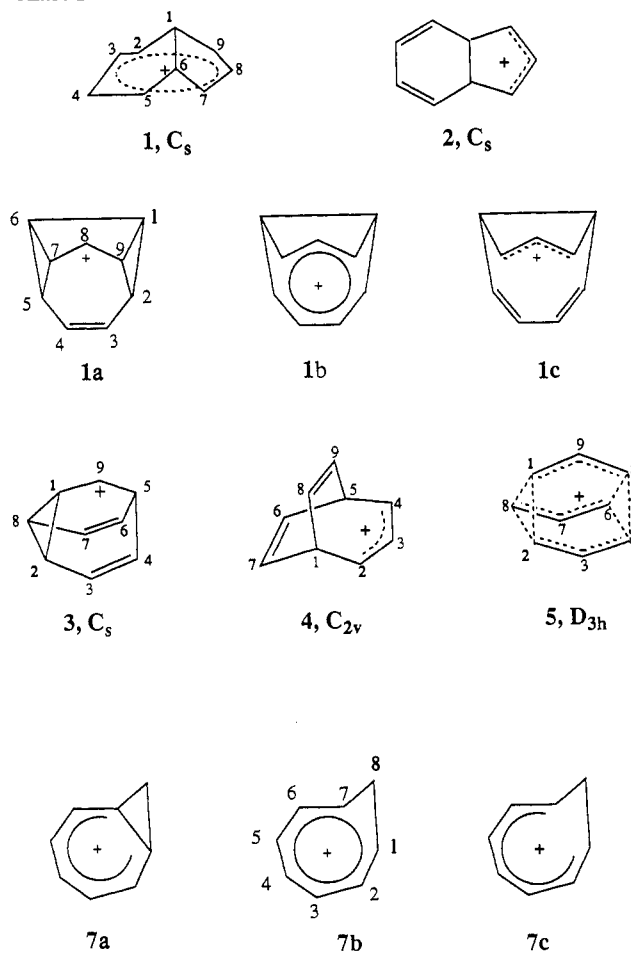
**Abstract:** The potential energy surface (PES) of  $C_9H_9^+$  has been investigated in the region of the 1,4-bishomotropylium cation (**1**) and its classical analogue, the *cis*-8,9-dihydro-1-indenyl cation (**2**) using second-, third-, and fourth-order Møller-Plesset perturbation theory (MP2, MP3, MP4(SDQ)) in connection with a 6-31G(d) basis set. Calculations show that **1** rather than **2** corresponds to a minimum-energy structure, contrary to recent Hartree-Fock results. Ion **1** is clearly bishomoaromatic with interaction distances of 2.1 Å. Its homoaromatic character is reflected by bond and charge equalization in its seven-membered ring, by a similar equalization of calculated IGLO/6-31G(d)  $^{13}C$  chemical shifts, and by MP2/6-31G(d) CC bond orders typical of aromatic delocalization of  $6\pi$  electrons. Since the PES is rather flat in the vicinity of **1** and since the homoaromatic stabilization energy is (with ca. 3 kcal/mol) rather small, perturbations due to substituents, counterions, or media may easily weaken homoaromaticity in **1**. A detection of the homoaromatic character of **1** and its derivatives is best carried out by  $^{13}C$  NMR measurements while energy-related measurements are probably not sensitive enough to confirm homoaromaticity for **1**.

## 1. Introduction

In this paper, we investigate structure, stability, magnetic properties, and bonding of the 1,4-bishomotropylium cation (**1**) and its classic analogue, the *cis*-8,9-dihydro-1-indenyl cation (**2**, see Chart I). Our investigation is the second step of a computational exploration of those parts of the potential energy surface (PES) of  $C_9H_9^+$  that host bicyclic and tricyclic cations with peculiar chemical properties. In the previous paper,<sup>1</sup> we have investigated the 9-barbaralyl cation (**3**) and its degenerate rearrangements which pass through cations **4** and **5** (Chart I). Now, we will concentrate on **1** and clarify whether **1** is an example of a bishomoaromatic (bis-ha) compound. For this purpose, we will apply techniques which we have successfully used in two previous studies.<sup>2,3</sup>

The concept of homoaromaticity has stimulated numerous synthetic, spectroscopic, and mechanistic studies in organic chemistry ever since it was first advanced by Winstein more than three decades ago.<sup>4-6</sup> It has been used to rationalize relative stability, geometry, spectroscopic properties, and kinetic behavior of molecules in which an aromatic  $\pi$  system is interrupted by an aliphatic fragment. So far homoaromatic (ha) character has been invoked for cations, anions, and neutral molecules, where

Chart I



<sup>†</sup> Department of Theoretical Chemistry.

<sup>‡</sup> Department of Organic Chemistry.

(1) Part I: previous paper in this issue.

(2) Cremer, D.; Reichel, F.; Kraka, E. *J. Am. Chem. Soc.* **1991**, *113*, 9459.

(3) Svensson, P.; Reichel, F.; Ahlberg, P.; Cremer, D. *J. Chem. Soc., Perkin Trans. 2* **1991**, 1463.

(4) Winstein, S. *J. Am. Chem. Soc.* **1959**, *81*, 6524.

(5) For reviews on homoaromaticity see: (a) Winstein, S. Q. *Rev. Chem. Soc.* **1969**, *23*, 141. (b) Warner, P. M. In *Topics in Nonbenzenoid Aromatic Character*; Nozoe, T.; Breslow, R.; Hafner, K.; Ito, S.; Murata, I., Eds.; Hirokawa: Tokyo, 1979; Vol. 2. (c) Paquette, L. A. *Angew. Chem., Int. Ed. Engl.* **1978**, *17*, 106. (d) Childs, R. F. *Acc. Chem. Res.* **1984**, *17*, 347. (e) Childs, R. F.; Mahendran, M.; Zweep, S. D.; Shaw, G. S.; Chadda, S. K.; Burke, N. A. D.; George, B. E.; Faggiani, R.; Lock, C. J. L. *Pure Appl. Chem.* **1986**, *58*, 111. (f) Haddon, R. C. *Acc. Chem. Res.* **1988**, *21*, 243.

(6) (a) Hehre, W. J. *J. Am. Chem. Soc.* **1974**, *96*, 5207. (b) Haddon, R. C. *Tetrahedron Lett.* **1974**, 2797, 4303. (c) Haddon, R. C. *Tetrahedron Lett.* **1975**, 863. (d) Haddon, R. C. *Tetrahedron Lett.* **1975**, 863. (e) Haddon, R. C. *J. Am. Chem. Soc.* **1975**, *97*, 3608. (f) Haddon, R. C. *J. Org. Chem.* **1979**, *44*, 3608. (g) Cremer, D.; Kraka, E.; Slee, T. S.; Bader, R. F. W.; Lau, C. D. H.; Nguyen-Dang, T. T. *J. Am. Chem. Soc.* **1983**, *105*, 5069. (h) Haddon, R. C. *J. Am. Chem. Soc.* **1988**, *110*, 1108.

in the latter two cases the notion of homoaromaticity is still a matter of controversial discussions.<sup>7</sup> In addition, it has been used to describe transition states of pericyclic reactions.<sup>8</sup>

There are two formal ways of constructing a potentially ha



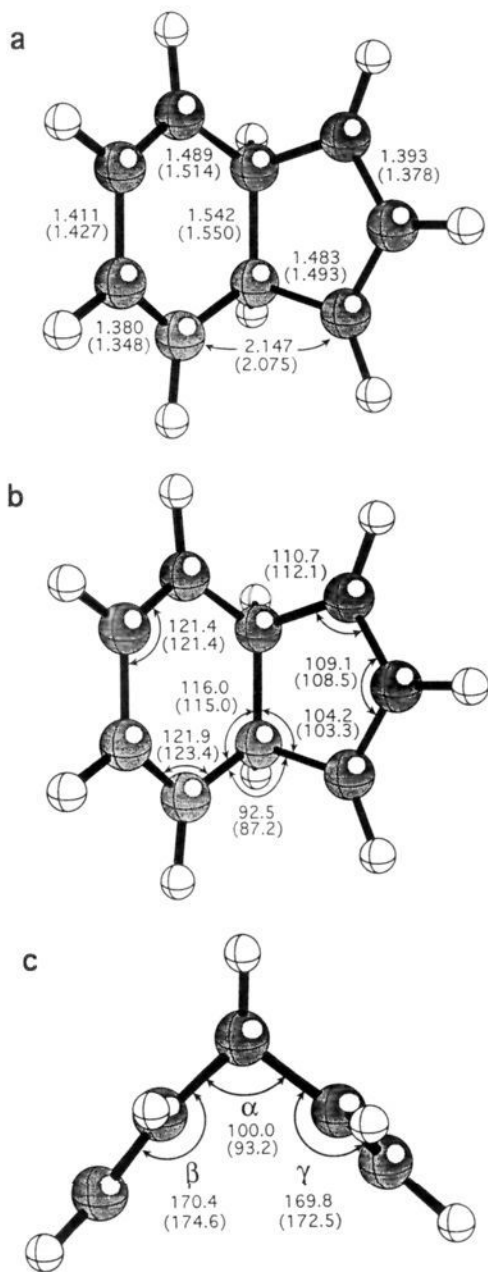


**Figure 1.** MP4(SDQ)-MP2/6-31G(d) geometry of the 1,4-bishomotropylum cation (**1b**) (see text): (a) bond lengths in Å; (b) bond angles in deg; (c) folding angles in deg. Numbers in parentheses give the HF/6-31G(d) geometry of **1b** obtained for a folding angle  $\alpha$  that was determined by IGLO/6-31G(d) calculations.<sup>3</sup>

**1a**, **1b**, and **1c** (**2**). This direction is best described by the folding angle  $\alpha$ , which upon enlargement leads to a continuous change in distances  $r(2,9)$  and  $r(6,7)$  (compare with Figure 1). After calculating MP2/6-31G(d) geometries for fixed values of  $\alpha$ , we have carried out MP3/6-31G(d)//- and MP4(SDQ)/6-31G(d)//MP2/6-31G(d) single-point calculations. MP4(SDQ)<sup>22</sup> compensates for some of the deficiencies of the MP2 approach and, accordingly, has led to a reliable description of the PES of  $C_9H_9^+$  in the vicinity of **3**.<sup>1</sup>

In the second step, we have carried out IGLO/6-31G(d) calculations of <sup>13</sup>C chemical shifts at MP2 geometries. IGLO (individual gauge for localized orbitals)<sup>23</sup> is known to lead to reasonable <sup>13</sup>C chemical shifts in the case of classical and nonclassical carbocations provided a reasonably accurate equilibrium geometry is available for the molecule in question.<sup>1-3,24,25</sup> Therefore, analysis of the differences between exper-

imental and calculated <sup>13</sup>C chemical shift values can lead to a fairly accurate structure determination. We have used this approach successfully in the case of **7**,<sup>2</sup> and therefore, we will test its usefulness also in the case of **1** and **2**.

Cremer and Kraka<sup>26</sup> have recently established two criteria for a density description of covalent bonds utilizing Bader's virial partitioning method of electron density distributions  $\rho(r)$ .<sup>27</sup> According to these authors, covalent bonding implies that the two nuclei in question are connected by a path of maximum electron density that is characterized by a [3, -1] critical point  $r_B$  (saddle point) along this path (necessary condition). At  $r_B$ , the calculated energy density  $H(r)$  must be stabilizing ( $H(r_B) < 0$ , sufficient condition).<sup>26</sup> Applying these criteria, numerous covalent bonds, both classical and nonclassical, have been investigated so far.<sup>28</sup> Therefore, we will use here the Cremer-Kraka definition of covalent bonding to answer the question whether a delocalization of electrons leads to a bond as predicted by Winstein. Besides the analysis of the electron density distribution, we will also investigate the Laplace concentration  $-\nabla^2\rho(r)$ ,<sup>26,29</sup> which provides information about depletion and concentration of negative charge and, therefore, can be used to detect strong through-space interactions. Both  $\rho(r)$  and  $-\nabla^2\rho(r)$  have been computed at the MP2/6-31G(d) level of theory using techniques published elsewhere.<sup>30,31</sup> Calculations have been performed on a CRAY XMP-416 using the COLOGNE90 ab initio package,<sup>32</sup> which includes an implementation of the IGLO method of Kutzelnigg and Schindler,<sup>33</sup> and the GAUSSIAN90 ab initio package.<sup>34</sup>

### 3. Energies and Geometries

Recently, Svensson and co-workers<sup>3</sup> have found that HF/6-31G(d) predicts **2** rather than **1** to correspond to a minimum-

(24) (a) Schindler, M. *J. Am. Chem. Soc.* **1987**, *109*, 1020. (b) Kutzelnigg, W.; Fleischer, U.; Schindler, M. *NMR: Basic Princ. Prog.* **1991**, *23*, 1.

(25) See, e.g.: (a) Hnyk, D.; Vajda, E.; Buehl, M.; Schleyer, P. v. R. *Inorg. Chem.* **1992**, *31*, 2464. (b) Buehl, M.; Schleyer, P. v. R. *J. Am. Chem. Soc.* **1992**, *114*, 477. (c) Buehl, M.; Schleyer, P. v. R.; McKee, M. L. *Heteroat. Chem.* **1991**, *2*, 499. (d) Buehl, M.; Schleyer, P. v. R. *Angew. Chem.* **1990**, *102*, 962. (e) Schleyer, P. v. R.; Buehl, M.; Fleischer, U.; Koch, W. *Inorg. Chem.* **1990**, *29*, 153. (f) Schleyer, P. v. R.; Koch, W.; Liu, B.; Fleischer, U. *J. Chem. Soc., Chem. Commun.* **1989**, 1098. (g) Bremer, M.; Schoetz, K.; Schleyer, P. v. R.; Fleischer, U.; Schindler, M.; Kutzelnigg, W.; Koch, W.; Pulay, P. *Angew. Chem.* **1989**, *101*, 1063.

(26) (a) Cremer, D.; Kraka, E. *Angew. Chem., Int. Ed. Engl.* **1984**, *23*, 627. (b) Cremer, D.; Kraka, E. *Croat. Chem. Acta* **1984**, *57*, 1259. (c) Kraka, E.; Cremer, D. In *Molecular Structure and Energetics, Structure and Reactivity*; Liebman, J. F., Greenberg, A., Eds.; VCH Publishers: New York, 1988; Vol. 7, p 65.

(27) (a) Bader, R. F. W.; Nguyen-Dang, T. T.; Tai, Y. *Rep. Prog. Phys.* **1981**, *44*, 893. (b) Bader, R. F. W.; Nguyen-Dang, T. T.; *Adv. Quantum Chem.* **1981**, *14*, 63. (c) Bader, R. F. W. In *The Force Concept in Chemistry*; Deb, B. M., Ed.; Van Nostrand Reinhold Company: New York, 1981; p 39.

(28) (a) Cremer, D. In *Modelling of structure and properties of molecules*; Maksic, Z. B., Ed.; Ellis Horwood: Chichester, England, 1988; p 125. (b) Cremer, D.; Gauss, J.; Schleyer, P. v. R.; Budzelaar, P. H. M. *Angew. Chem., Int. Ed. Engl.* **1984**, *23*, 370. (c) Cremer, D.; Kraka, E. *J. Am. Chem. Soc.* **1985**, *107*, 3800, 3811. (d) Cremer, D.; Gauss, J. *J. Am. Chem. Soc.* **1986**, *108*, 7467. (e) Cremer, D.; Bock, C. W. *J. Am. Chem. Soc.* **1986**, *108*, 3375. (f) Koch, W.; Frenking, G.; Gauss, J.; Cremer, D.; Sawaryn, A.; Schleyer, P. v. R. *J. Am. Chem. Soc.* **1986**, *108*, 5732. (g) Koch, W.; Frenking, G.; Gauss, J.; Cremer, D. *J. Am. Chem. Soc.* **1986**, *108*, 5808. (h) Budzelaar, P. H. M.; Cremer, D.; Wallasch, M.; Würthwein, E.-U.; Schleyer, P. v. R. *J. Am. Chem. Soc.* **1987**, *109*, 6290. (i) Koch, W.; Frenking, G.; Gauss, J.; Cremer, D.; Collins, J. R. *J. Am. Chem. Soc.* **1987**, *109*, 5917. (j) Cremer, D.; Kraka, E. In *Molecular Structure and Energetics, Structure and Reactivity*; Liebman, J. F., Greenberg, A., Eds.; VCH Publishers: Deerfield Beach, FL, 1988; Vol. 7, p 65. (k) Cremer, D. *Tetrahedron* **1988**, *44*, 7427. (l) Cremer, D.; Gauss, J.; Kraka, E. *THEOCHEM* **1988**, *169*, 531. (m) Frenking, G.; Koch, W.; Reichel, F.; Cremer, D. *J. Am. Chem. Soc.* **1990**, *112*, 4240. (n) Frenking, G.; Cremer, D. *Struct. Bonding* (Berlin) **1990**, *73*, 17.

(29) (a) Bader, R. F. W.; Essén, H. *J. Chem. Phys.* **1984**, *80*, 1943. (b) Bader, R. F. W.; MacDougall, P. J.; Lau, C. D. H. *J. Am. Chem. Soc.* **1984**, *106*, 1594. (c) Bader, R. F. W.; MacDougall, P. J. *J. Am. Chem. Soc.* **1985**, *107*, 6788.

(30) Kraka, E.; Gauss, J.; Cremer, D. *THEOCHEM* **1991**, *234*, 95. (31) (a) Gauss, J.; Cremer, D. *Adv. Quantum Chem.* **1992**, *23*, 205. (b) Gauss, J.; Cremer, D. *Chem. Phys. Lett.* **1987**, *138*, 131. (c) Gauss, J.; Cremer, D. *Chem. Phys. Lett.* **1988**, *153*, 303.

(32) Gauss, J.; Kraka, E.; Reichel, F.; Cremer, D. *COLOGNE90*; University of Göteborg: Göteborg, Sweden, 1990.

(33) Kutzelnigg, W.; Schindler, M.; van Wüllen, C. *IGLO*; University of Bochum: Bochum, Sweden, 1989.

(34) Frisch, M. J.; Head-Gordon, M.; Trucks, G. W.; Foresman, J. B.; Schlegel, H. B.; Raghavachari, K.; Robb, M. A.; Binkley, J. S.; Gonzalez, C.; Defrees, D. J.; Fox, D. J.; Whiteside, R. A.; Seeger, R.; Melius, C. F.; Baker, J.; Martin, R. L.; Kahn, L. R.; Stewart, J. J. P.; Topiol, S.; Pople, J. A. *Gaussian 90*; Gaussian, Inc.: Pittsburgh, PA, 1990.

(22) Krishnan, R.; Pople, J. A. *Int. J. Quantum Chem.* **1978**, *14*, 91.

(23) (a) Kutzelnigg, W. *Isr. J. Chem.* **1980**, *19*, 193. (b) Schindler, M.; Kutzelnigg, W. *J. Chem. Phys.* **1982**, *76*, 1919.

**Table I.** MP2/6-31G(d) Geometries of Cations **1** and **2**<sup>a</sup>

parameter	<b>1a</b>	<b>1b</b>	<b>1c (2)</b>
$\alpha$	70.0	86.6	113.8
$\beta$	-169.0	177.5	172.7
$\gamma$	-176.0	174.0	171.5
$r(2,9)$	1.658	1.933	2.356
$r(1,2)$	1.516	1.490	1.507
$r(2,3)$	1.413	1.391	1.357
$r(3,4)$	1.376	1.395	1.442
$r(1,6)$	1.528	1.537	1.545
$r(1,9)$	1.532	1.495	1.477
$r(7,8)$	1.399	1.396	1.390
$\angle(2,1,9)$	65.9	80.7	104.3
$\angle(2,1,6)$	114.8	115.6	116.3
$\angle(6,1,9)$	105.0	104.6	103.7
$\angle(1,2,3)$	124.0	123.3	121.3
$\angle(2,3,4)$	120.2	121.0	122.0
$\angle(1,9,8)$	109.0	110.0	112.1
$\angle(7,8,9)$	112.0	110.3	107.7

<sup>a</sup> Bond lengths in Å, angles in deg. For the definition of angles  $\alpha$ ,  $\beta$ , and  $\gamma$ , see Figure 1.

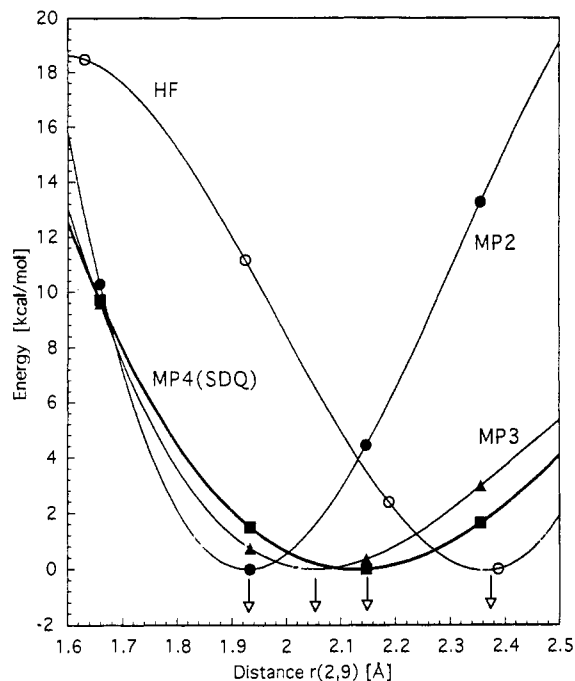


**Figure 2.** HF/-, MP2/-, MP3/-, and MP4(SDQ)/6-31G(d) PES of  $C_9H_9^+$  in the direction connecting structures **1a**, **1b**, and **1c (2)**. This direction can be defined either by the folding angle  $\alpha$  or the distance  $r(2,9)$ . Position of minimum is indicated in each case by an arrow.

energy structure of  $C_9H_9^+$ . Here, we present evidence that this result is an artifact of HF theory. MP2/6-31G(d) geometry optimizations (Table I) lead to a minimum that clearly corresponds to **1b** with an  $r(2,9)$  distance of 2.1 Å ( $\alpha = 86.6^\circ$ ). A similar interaction distance has been found for **7b** (Chart I) at the same level of theory.<sup>2</sup> Structures **1a** and **1c (2)**<sup>35</sup> are 10.3 and 13.2 kcal/mol higher in energy and do not correspond to stationary points on the MP2/6-31G(d) PES of  $C_9H_9^+$ , as becomes obvious by inspection of Figure 2, which depicts the PES along the search direction **1a**–**1c**.

MP3/6-31G(d) and MP4(SDQ)/6-31G(d) qualitatively confirm the MP2 result but suggest that the equilibrium value of  $\alpha$  is shifted toward the HF value of **2** ( $\alpha = 113.8^\circ$ ,  $r(2,9) = 2.4 \text{ \AA}$ ). At MP4(SDQ),  $\alpha$  is close to  $100^\circ$ , corresponding to an interaction distance  $r(2,9)$  of 2.14 Å. Going from MP2 to MP4(SDQ), the

(35) Since structures **1a** and **1c** do not correspond to stationary points on the PES, we have made the (arbitrary) choice of modeling **1a** by a form for which bonds C2–C9 and C5–C7 are just about to be formed ( $\alpha = 70^\circ$ ) and **1c** by the geometry obtained for **2** at the HF/6-31G(d) level of theory.<sup>3</sup>

**Table II.** Magnetic Properties of Ions **1a**, **1b**, and **1c (2)** Calculated at the IGLO/6-31G(d) Level of Theory<sup>a</sup>

parameter	<b>1a</b> MP2 <sup>b</sup>	<b>1c (2)</b> MP2 <sup>b</sup>	<b>1b</b> MP4-MP2 <sup>b</sup>	expt
$\delta(C1)$	52.4	46.4	45.9	52.6
$\delta(C2)$	72.2	121.1	121.5	117.2
$\delta(C3)$	141.7	141.9	145.4	140.2
$\delta(C7)$	69.3	227.4	176.9	155.5
$\delta(C8)$	212.8	148.3	145.4	144.0
$-\chi$	101.0	83.3	97.0	

<sup>a</sup> Chemical shifts  $\delta(C)$  in ppm relative to  $(CH_3)_4Si$ ; magnetic susceptibility  $-\chi$  in  $10^{-6} \text{ cm}^3 \text{ mol}^{-1}$ . For numbering of atoms, see Chart I. Experimental values from ref 12b. <sup>b</sup> Geometry calculated at the MPn/6-31G(d) level of theory.

PES becomes flatter, suggesting that **1b** can carry out large amplitude vibrations which correspond to an opening and closing to the folding angle  $\alpha$  between five- and six-membered rings. A relatively small energy increase of about 2 kcal/mol has **1b** swinging in the region  $r(2,9) = 1.9$ – $2.4 \text{ \AA}$  (MP4(SDQ)/6-31G(d) PES, see Figure 2). However, an energy increase of about 10 kcal/mol is necessary to reach structure **1a**.

These observations are similar to those made by Cremer and co-workers<sup>2</sup> in the case of **7b**, for which a (harmonic) force constant of just 0.2 mdyne/Å (MP4(SDQ)/6-31G(d)) for large-amplitude vibrations in the direction of the 1,7 distance was calculated. The corresponding value for **1b** is 0.45 mdyne/Å, which suggests that **1b** is somewhat more rigid than **7b**. Also, interactions in **1b** seem to be somewhat weaker than those in **7b** if one considers that interaction distances differ by 0.1 Å in the two ions (2.03 Å for **7b**,<sup>2</sup> 2.14 Å for **1b**, MP4(SDQ)/6-31G(d)). Both observations are not astonishing in view of the fact that a transition from structure **b** to structure **a** should build up almost twice as much strain in the case of **1** (two three-membered rings are formed) as in the case of **7**.

We have reoptimized the geometry of **1** at the MP2/6-31G(d) level utilizing the MP4(SDQ)/6-31G(d) value of  $\alpha$ . The resulting geometry (shown in Figure 1) clearly reflects the high degree of bond equalization which is obtained in the seven-membered ring C2, C3, C4, C5, C7, C8, C9 (1.38, 1.41, 1.38, 1.39, 1.39 Å, Figure 1). Since both **1a** and **1c (2)** show significant bond alternation in the seven-membered ring, we can use the degree of bond equalization calculated for **1b** and the fact that all bond lengths are close to a typically aromatic distance of 1.40 Å as one indication of bis-ha character for **1**.

According to MP4(SDQ)/6-31G(d) energies, **1** is 8.3 kcal/mol more stable than the barbaralyl cation **3** (compare with Table V of ref 1) and, thereby, **1** is the most stable bicyclic  $C_9H_9^+$  ion. Since a free activation enthalpy of 10.4 kcal/mol has been found at  $-125^\circ\text{C}$  for the rearrangement of **3** to **1**,<sup>13</sup> the reverse process will require close to 19 kcal/mol, i.e., under the conditions of the experiment the rearrangement of **3** to **1** should be irreversible, which is in line with the experimental findings.

#### 4. Magnetic Properties

The <sup>13</sup>C NMR spectrum of **1** has been measured, and all NMR signals could be assigned (see Table II).<sup>11–14</sup> Therefore, it was challenging to calculate IGLO <sup>13</sup>C NMR shift values for all structures investigated and to compare them with the experimental data. IGLO/6-31G(d) <sup>13</sup>C chemical shifts as well as magnetic susceptibilities are listed in Table II, and the former are plotted as a function of distance  $r(2,9)$  in Figure 3. Figure 3 shows that <sup>13</sup>C chemical shifts of the bridge atoms C1 and C6 do only weakly depend on the distance  $r(2,9)$  and the folding angle  $\alpha$ . Even weaker is the dependence of the shift value for C3 and C4 while all other shifts strongly depend on  $r(2,9)$  and  $\alpha$ .

These trends are easily understood when considering the structural changes for the rearrangement from **1a** to **1c** (see Chart I) and comparing them with the corresponding changes

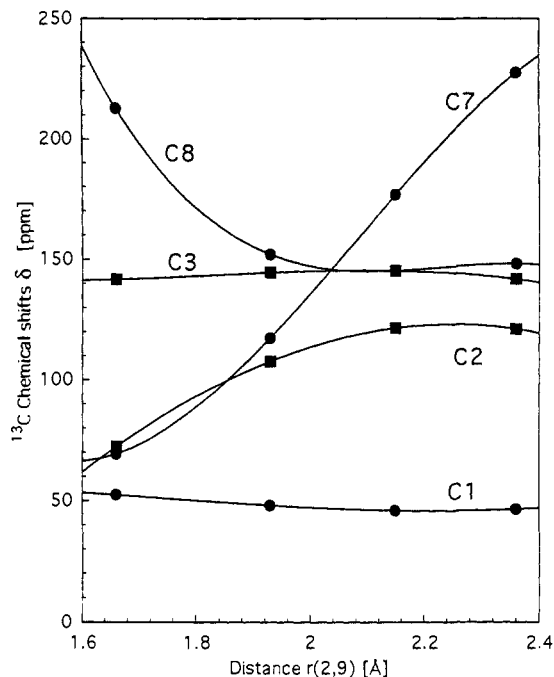


**Figure 3.** IGLO/6-31G(d)//MP2/6-31G(d)  $^{13}\text{C}$  chemical shifts  $\delta$  given as a function of the distance  $r(2,9) = r(5,7)$ . For the corresponding  $\alpha$ -values, see Table I.

of MP2/6-31G(d) gross atomic charges. When going from **1a** to **1c**, the bridge bond becomes only slightly longer because of some rehybridization at C1 and C6 (change from a cyclopropane hybridization to normal  $\sigma$ -bond hybridization). Apart from this, the bridge atoms are not involved in the electronic changes that occur in the periphery of the seven-membered ring when going from **1a** to **1c**. These changes should be largest at the interaction centers C2, C5, C7, and C9. Accordingly, a strong variation in the shift values is found for atoms C2 (C5) and C7 (C9). The corresponding nuclei become deshielded upon opening of the three-membered-ring bonds, which is in line with a delocalization of positive charge. As a consequence, the positive charge at C8, which is highly localized in **1a**, decreases, thus leading to a shielding of the nucleus C8 (see Figure 3). Figure 3 also shows that charge delocalization upon enlargement of  $r(2,9)$  does not affect so much C3 and C4, the shift values of which remain fairly constant (Figure 3).

Since three of the five  $^{13}\text{C}$  chemical shifts show a clear dependence on the distance  $r(2,9)$ , it is possible to determine the equilibrium value of  $r(2,9)$  and the folding angle  $\alpha$  by comparing for each structure investigated calculated shift values with those measured for **1**. In Figure 4, the calculated mean deviation  $\Delta = \sum|\delta(\text{exp}) - \delta(\text{theor})|/9$  is given as a function of distance  $r(2,9)$ . The minimum of  $\Delta$  (7.8 ppm) is obtained for  $r(2,9) = 2.1 \text{ \AA}$ , which is close to the MP4(SDQ)/6-31G(d) value of  $r(2,9)$  (see Figure 1). Hence, the experimentally observed  $\text{C}_9\text{H}_9^+$  cation must possess structure **1b**.

### 5. Bishomoaromaticity of **1**—Fact or Fiction?

Aromatic, antiaromatic, homoaromatic, etc. character of a molecule can only be quantified if appropriate reference molecules are defined. Actually, a molecule can only function as a reference if it does not possess the molecular property to be investigated but apart from this has exactly the same electronic features as the target molecule. In most cases, such a system is hard to find, in particular if one is limited by the hardships of experiment. As a consequence, experimentalists tend to use badly suited reference compounds that require a lot of additional assumptions and, therefore, cannot aid a reliable description of the target molecule. In theory, the definition of a reference state is often easier, since

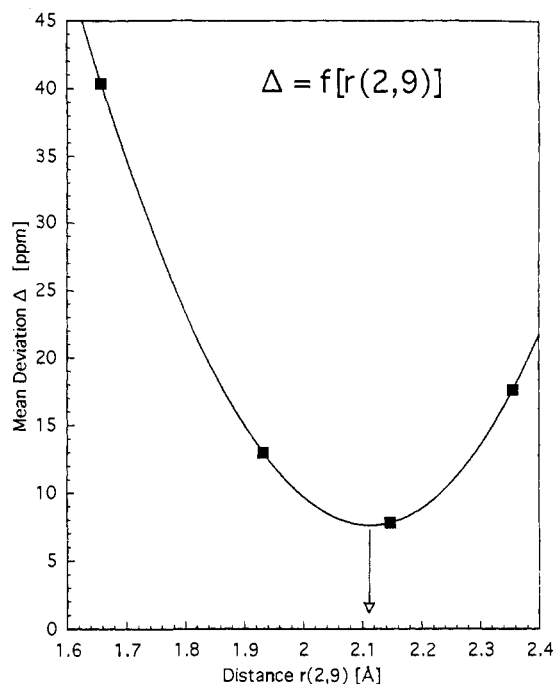


**Figure 4.** Mean deviation  $\Delta$  of IGLO/6-31G(d)//MP2/6-31G(d)  $^{13}\text{C}$  chemical shifts from experimental values of **1** given as a function of distance  $r(2,9) = r(5,7)$ . For the corresponding  $\alpha$ -values, see Table I. The minimum of the mean deviation is indicated by an arrow.

theory is not bound by the limitations of experiment. Nevertheless, it is difficult, not to say impossible, to define a reference state that possesses exactly the same strain energy as **1** but does not benefit from ha interactions. Clearly, **1a** cannot be such a reference state, since its strain energy should be much higher than that of **1b**. In this respect, **1c** might seem to be a better reference; but **1c** with an interaction distance  $r(2,9) = 2.36 \text{ \AA}$  will definitely be stabilized by through-space interactions, and accordingly, the potential ha stabilization energy of **1b** will be somewhat underestimated when using **1c** as a reference.

Therefore, we will set back the question of the stabilization energy of **1** for the moment and instead will list those properties of **1** that make its bis-ha character more than likely. (1) As shown in Figure 1, the equilibrium geometry of **1** corresponds neither to **1a** nor to **1c**. Instead it is equal to **1b**, which, in case of identical geometries, could be considered as a resonance hybrid of **1a** and **1c**. (2) For the equilibrium geometry **1b**, maximal bond equalization is obtained in the seven-membered ring formed by atoms C2, C3, C4, C5, C7, C8, and C9 (see Table I), as it is found for **7b** and aromatic compounds in general.<sup>2</sup> (3) In **1b** the positive charge is strongly delocalized, which is clearly different from situations **1a** and **1c** (see Figure 5). As a consequence, the gross atomic charges of the seven ring atoms are largely equalized. For example, the positive charge at C8H is only 0.1 electron larger than that of the other CH groups in the seven-membered ring. The bridge (C1H–C6H), however, does not participate in the charge delocalization and, accordingly, is uncharged. Again, these observations are typical of aromatic (and ha) compounds. (4)  $^{13}\text{C}$  chemical shift values of **1** are parallel to calculated atomic charges (compare Figures 3 and 5), i.e., for **1b** a maximal equalization of chemical shifts is obtained. This seems to be typical of ha compounds, since Cremer and co-workers have made the same observation for **7b**.<sup>2</sup> (5) IGLO/6-31G(d) magnetic susceptibilities of **1a**, **1b**, and **1c** (Table II), if plotted in dependence of  $r(2,9)$ , reach a maximum value close to  $1.9 \text{ \AA}$ , which seems to be the point of maximum delocalization of the  $6\pi$  electrons along the periphery of the seven-membered ring of **1b**. (6) MP2/6-31G(d) bond orders<sup>36</sup> (Figure 7) also indicate that  $6\pi$  electron delocalization is largest for  $r(2,9) = 1.9 \text{ \AA}$  but still large for the MP4(SDQ) equilibrium value of  $r(2,9)$ .

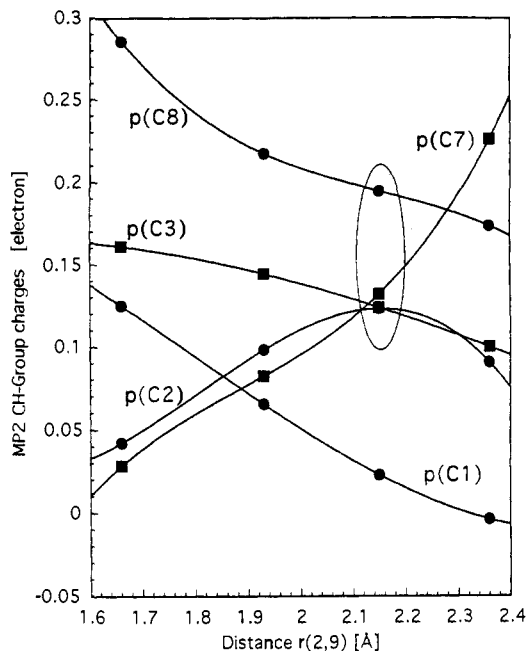


**Figure 5.** MP2/6-31G(d) gross atomic charges of CH groups given as a function of distance  $r(2,9) = r(5,7)$ . For the corresponding  $\alpha$ -values, see Table I. Charges obtained for the seven-membered ring of **1b** at its equilibrium geometry are indicated.

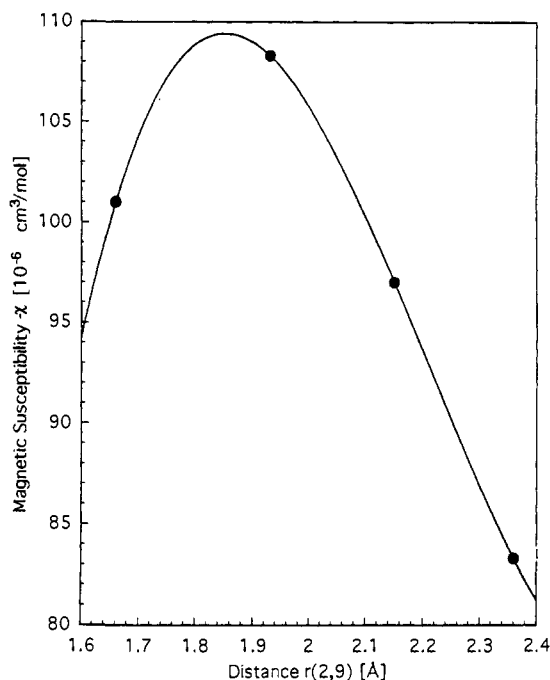


**Figure 6.** IGLO/6-31G(d,p) magnetic susceptibility  $-\chi$  given as a function of distance  $r(2,9) = r(5,7)$ . For the corresponding  $\alpha$ -values, see Table I.

Observations 1–6 establish the bis-ha character of **1b** beyond any doubt, and therefore, it is safe to say that **1** is a bis-ha prototype in the same way as **7b** is the mono-ha prototype. By-and-large, the properties of **1b** and **7b** are similar, even though the ha interaction distance is somewhat larger (2.14 vs 2.03 Å) and the degree of bond, charge, and shift equalization somewhat smaller in **1b** than in **7b**. This not astonishing, since strain should be significantly larger in **1b** than in **7b**. In both molecules, the highest

(36) Bond orders  $n$  have been calculated from the equation  $n = \exp[A\{\rho(r_B) - B\}]$  where  $\rho(r_B)$  denotes the electron density at the bond critical point  $r_B$  and constants  $A$  and  $B$  have been determined from MP2/6-31G(d) response densities at the CC bond critical points of ethane and ethylene. See ref 26.

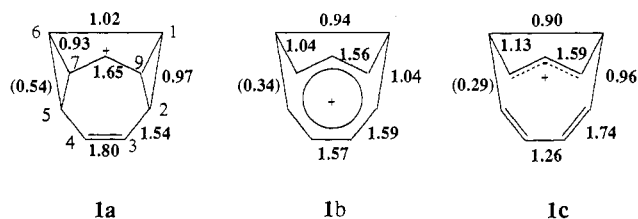


**Figure 7.** MP2/6-31G(d) CC bond orders  $n^{26}$  of **1a**, **1b**, and **1c** (2).<sup>35</sup> Numbers in parentheses measure the buildup of electron density between nonbonded atoms, and therefore, they provide a quantitative indicator of the strength of through-space interactions. They have been determined by using the bond order formula<sup>36</sup> for the MP2/6-31G(d) electron density at the midpoint between C5 (C2) and C7 (C9).

degree of aromatic  $6\pi$  delocalization seems to be reached at an interaction distance of about 1.9 Å, but in order to avoid molecular strain, in particular ring strain, the seven-membered rings open to an interaction distance of 2.03 (**7b**)<sup>2</sup> and 2.14 Å (**1b**), respectively. It is easy to foresee a situation where enhanced strain will lead to further opening of the ha cycle until homoaromaticity becomes too weak to be an important factor. Accordingly, ha character seems to be always a delicate balance between (destabilizing) strain effects and (stabilizing)  $\pi$ -delocalization effects with a small preference for the latter.

*Does 1b possess an ha bond in the way Winstein has discussed it?* Investigation of the electron density distribution  $\rho(r)$  of **1b** along the lines described by Cremer and Kraka<sup>26</sup> reveals that there is no path of maximum electron density between centers 2 (5) and 9 (4) and, accordingly, the necessary criterion for a covalent bond is not fulfilled. Covalent bonds C2–C9 and C4–C5 are lost as **1** passes through **1a** on the way to **1b** and **1c**. This is nicely reflected by the perspective drawings of the MP2/6-31G(d) Laplace concentration,  $-\nabla^2\rho(r)$ , shown in Figure 8 for the plane of the three nuclei of C1, C2, and C9. For **1a** (Figure 8a), an enhanced electron concentration in the internuclear region C2–C9 is still visible and does indicate that the bond C2–C9 has just been broken. In the case of **1c** (Figure 8c), deep holes in the valence-electron concentration of C2 and C9 have formed at those locations (indicated by arrows in Figure 8c) that formerly were the locations of bond path and enhanced electron concentration. While the lumps in the valence-shell concentration of an atom are the positions of bond and lone electron pair concentrations, the holes in between point in the nonbonded directions and determine the positions of an electrophilic attack.<sup>27,28</sup>

Comparison of parts b and c of Figure 8 reveals that **1b** possesses the same valence shell holes as **1c** does, but the holes at C2 and C9 are not as deep as in the case of **1c**. There is already a small buildup of electron concentration in the direction of C2–C9, which is indicative of enhanced through-space interactions. This is confirmed by the calculated  $\rho(r)$  value at the midpoint of C2–C9, which is already 30% of that of a typical CC  $\sigma$ -bond. We conclude that ha electron delocalization in the case of **1b** is not the matter of the formation of an ha bond but of increased through-space interactions that lead to polarization of electronic charge in the direction of the interacting centers. This finding seems reasonable in view of the fact that bond formation, even though it should stabilize the molecule, will also increase molecular strain by that amount that results from the new cyclopropane units in **1b** or **7b**.

*Can we exclude homoaromaticity for structures such as 6a and 6c (Scheme I) on the basis of these findings?* The barbaralyl cation **3** (Chart I) investigated in part 1<sup>1</sup> contains in its periphery a potential  $6\pi$  system that via C2, C8 (CC bond distance 1.458 Å) and C4, C6 (CC nonbonded distance 2.400 Å) could delocalize, thus forming an ha system. However, according to our six criteria given above, ha character can be clearly excluded for **3**. In Figure 9, just as an example, the dependence of calculated <sup>13</sup>C chemical shifts is given in dependence of the interaction distance  $r(4,6)$ . At no point do the shift values of atoms C2, C3, C4, C6, C7, and

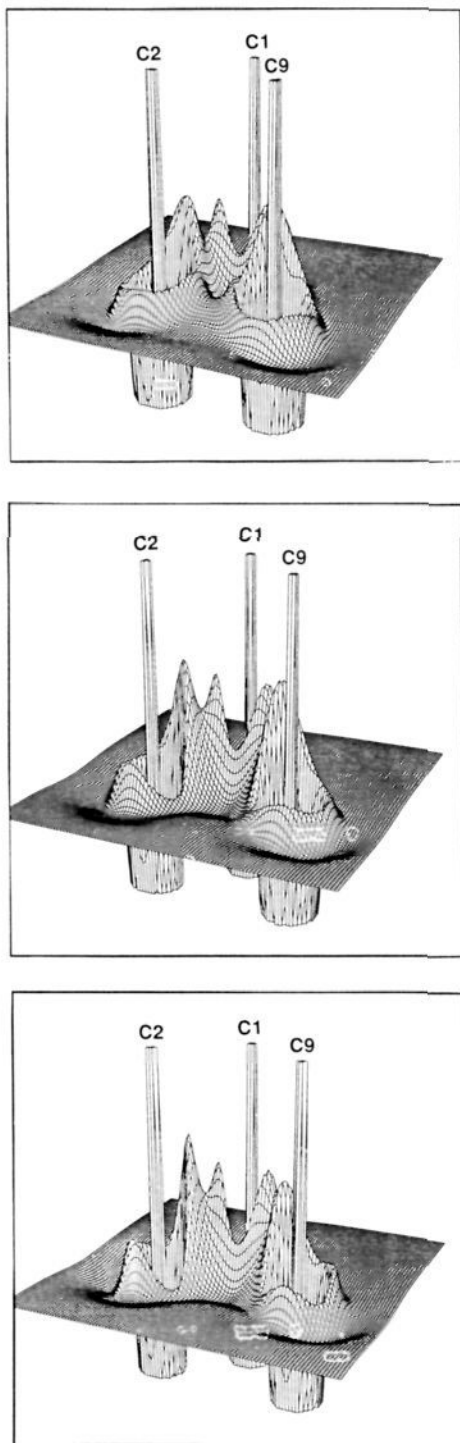


**Figure 8.** Perspective drawings of the MP2/6-31G(d) Laplace concentration  $-\nabla^2\rho(r)$  calculated for the plane containing atoms C1, C2, and C9 of (a) **1a**, (b) **1b**, and (c) **1c** (**2**).<sup>35</sup>

C8 in the potentially *ha* six-membered ring equalize or approach each other, thus indicating *ha* delocalization of electrons. This is also true for structure **5**, which actually possesses a delocalized electron system. But delocalization of electrons takes place in three dimensions and, thus, leads to a probably destabilized anti-cycloaromatic system.<sup>37</sup>

In view of our results, it is not likely that structures such as **6a** and **6c** (Scheme I) lead to any *ha* character. It seems that

(37) (a) Goldstein, M. J.; Hoffmann, R.; *J. Am. Chem. Soc.* **1971**, *93*, 6193. See also: (b) Goldstein, M. J. *J. Am. Chem. Soc.* **1967**, *89*, 6357. (c) Goldstein, M. J.; Odell, B. G. *J. Am. Chem. Soc.* **1967**, *89*, 6356.

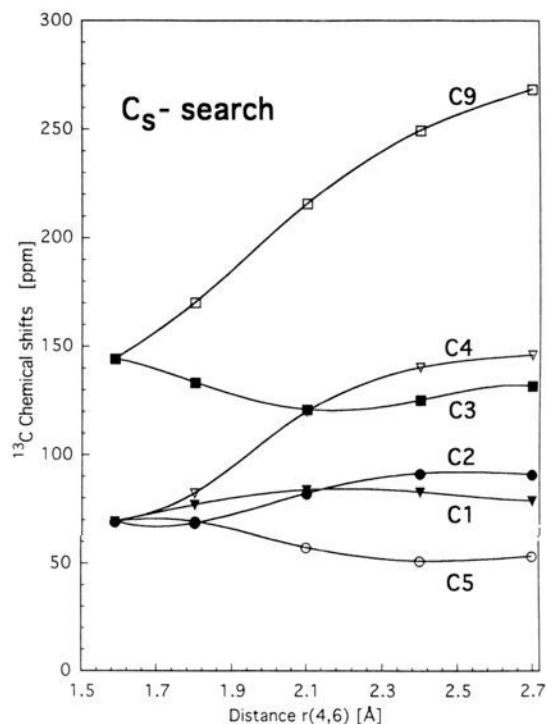


**Figure 9.** IGLO/6-31G(d)//MP2/6-31G(d)  $^{13}\text{C}$  chemical shifts  $\delta$  of cations **3** and **5** given as a function of the distance  $r(2,8) = r(4,6)$ .

this will be strongest for distances close to 2 Å. However, it is difficult to predict at what interaction distances, either larger or smaller than 2 Å, homoaromaticity ceases to be of any importance for the understanding of the properties of the molecule in question. This will depend more or less on the antenna used to measure these properties and the way to interpret them.

It remains to investigate the energetic consequences of homoaromaticity in **1b**. Cremer and co-workers<sup>2</sup> have found for **7b** an *ha* stabilization energy of just 4 kcal/mol. Inspection of Figure 1 shows that just 2 kcal/mol are needed to increase the *ha* interaction distance of **1b** from 2.14 to 2.4 Å, which is the value found for **3**. Since there exist at 2.4 Å still some through-space interactions (see above), it is reasonable to assume an *ha* stabilization energy of about 3–4 kcal/mol for **1b**.

## 6. Conclusions

The following conclusions can be drawn from this investigation.

- (1) Contrary to previous HF results,<sup>3</sup> the nonclassical 1,4-bishomotropylium cation (**1b**) rather than the classical *cis*-8,9-dihydro-1-indenyl cation (**2**) corresponds to a minimum-energy structure on the  $\text{C}_9\text{H}_9^+$  PES. Ion **1b** is 8.3 kcal/mol more stable than the 9-barbaralyl cation (**3**), which sits at another local minimum of the  $\text{C}_9\text{H}_9^+$  PES.
- (2) Ion **1b** is bis-*ha*, which is reflected by (a) typical *ha* interaction distances of 2.1 Å, that close a seven-membered ring constituted by atoms C2, C3, C4, C5, C7, C8, and C9; (b) a large degree of bond equalization in the seven-membered ring with MP2/6-31G(d) bond lengths of  $1.40 \pm 0.01$  Å; (c) a large degree of charge delocalization in the seven-membered ring that gives each CH group but C3H (0.2 e) a positive MP2/6-31G(d) charge of 0.12 e; (d) a similarly strong equalization of IGLO/6-31G(d)  $^{13}\text{C}$  chemical shifts in the seven-membered ring; (e) a maximum of the magnetic susceptibility  $-\chi = f(r(2,9))$  close to the  $r(2,9)$  equilibrium value of **1b**; and (f) MP2/6-31G(d) bond orders typical of an aromatic system and indicative of the delocalization of a  $6\pi$  electron ensemble.
- (3) Even though **1b** is bis-*ha*, it does not possess *ha* bonds between atoms C2,C9 and C4,C5. There is no path of maximum electron density between these centers, which according

to Cremer and Kraka<sup>26</sup> is a necessary condition for covalent bonding. The absence of an ha bond is confirmed by the MP2/6-31G(d) Laplace concentration that shows no substantial accumulation of negative charge in the interatomic region. (4) Both electron density distribution and Laplace concentration reveal a polarization of electronic charge between the interacting centers which is typical of strong through-space interactions. (5) The ha stabilization energy of **1b** is estimated to be just 3–4 kcal/mol. The PES is very flat at the location of **1b**, which means that a relatively small energy increase leads to relatively large changes in geometry. It is likely that **1b** carries out a large-amplitude vibration in the direction defined by the folding angle  $\alpha$ . (6) Because of the small ha stabilization energy of **1b**, it will be very difficult to measure any energetic consequences by experimental means. NMR spectroscopy should be a definitely much better method to detect the ha character of **1b** and its derivatives. (7) The observations made for **1b** are parallel to those recently found for **7b**,<sup>2</sup> and therefore, it is likely that homoaromaticity is often connected to ha interaction distances

close to 2 Å. The inherent strain of the molecule in question seems to decide whether the actual interaction distance is somewhat larger (large strain) or somewhat smaller (low strain). (8) Since homoaromaticity is a delicate balance between (destabilizing) strain and (stabilizing) through-space interactions, it will be interesting to check whether perturbations due to substituent, counterion, or media effects easily disrupt ha delocalization.<sup>38</sup> (9) It will be difficult to detect by either experimental or theoretical means the smooth transition from ha interactions (**6b**, Scheme I) to either bonded interactions as in **6a** or weak through-space interactions as in **6c**. Work is in progress to focus on this question.

**Acknowledgment.** This work was supported by the Swedish Natural Science Research Council (NFR). All calculations were done on the CRAY XMP/416 of the Nationellt Superdatorcentrum (NSC), Linköping, Sweden. The authors thank the NSC for a generous allotment of computer time.

---

(38) Cremer, D.; Svensson, P.; Kraka, E. To be published.